https://doi.org/10.1130/G51905.1

Manuscript received 22 November 2023 Revised manuscript received 14 February 2024 Manuscript accepted 19 March 2024

Published online 26 March 2024

© 2024 The Authors. Gold Open Access: This paper is published under the terms of the CC-BY license.

Rehydrated glass embayments record the cooling of a Yellowstone ignimbrite

Kenneth S. Befus^{1,*}, James O. Thompson¹, Chelsea M. Allison¹, Anna C. Ruefer¹, and Michael Manga²
¹Department of Geosciences, Baylor University, Waco, Texas 76798, USA
²Department of Earth and Planetary Science, University of California–Berkeley, Berkeley, California 94720-4767, USA

ABSTRACT

Hydration fronts penetrate 50–135 µm into glassy rhyolite embayments hosted in quartz crystals from the Mesa Falls Tuff in the Yellowstone Plateau volcanic field. The hydration fronts occur as steep enrichments that reach 2.4 ± 0.6 wt% H_2O at the embayment opening, representing much higher values than interior concentrations of 0.9 ± 0.2 wt% H_2O . Molecular water accounts for most of the water enrichment. Water speciation indicates the hydration fronts comprise absorbed meteoric water that modified the original magmatic composition of the rhyolitic glass. We used finite difference diffusion models to demonstrate that glass rehydration was likely produced over a few decades as the ignimbrite cooled. Such temperatures and time scales are consistent with rare firsthand observations of decadal hydrothermal systems associated with cooling ignimbrites at Mount Pinatubo (Philippines) and the Valley of Ten Thousand Smokes (Alaska).

INTRODUCTION

Volcanic glasses rehydrate when exposed to moisture. Rehydration is a diffusion-limited process that produces concentration gradients of water that become enriched at interfaces exposed to water. The shape and magnitude of water enrichment in a concentration gradient are functions of many variables, including water diffusivity, water solubility, glass composition, temperature, and time. Archaeologists were the first to exploit this relationship, using the thickness of hydration rinds on obsidian artifacts to establish the age of burial (e.g., Friedman and Smith, 1960; Liritzis and Laskaris, 2011). Geoscientists subsequently recognized that rehydration of natural glasses provides opportunities to reconstruct past geologic processes related to climate, hydrology, topography, tectonics, and volcanology (e.g., Cassel and Breecker, 2017; Mitchell et al., 2018; Hudak et al., 2021; McIntosh et al., 2022).

The use of rehydrated glass in volcanology requires careful assessment of water abundance and speciation because all volcanic glasses contain water. The source of water in volcanic glass may be primary magmatic, secondary meteoric, secondary marine, or combinations thereof.

Kenneth S. Befus https://orcid.org/0000-0003 -4636-7417

Magmatic melts contain dissolved water, with values commonly ranging between 0.1 and ~6 wt%. Dissolved magmatic water occurs as two separate species, molecular water and hydroxyl (Stolper, 1982). During eruption, both species of primary magmatic water exsolve during degassing, but they may also be partially preserved in erupted material by rapid ascent and quenching. The molecular water and hydroxyl preserved in erupted products record past volcanic processes because their relative proportions are controlled by intrinsic thermodynamic properties and kinetics. In contrast, low-temperature rehydration of rhyolite glass occurs almost entirely by diffusive absorption of molecular water. The resulting rehydration fronts occur as oversteepened, "S-shaped" concentration gradients (Anovitz et al., 2008; Hudak and Bindeman, 2020). The unique S-shaped form of the gradients is produced by the self-dependence of water diffusivity, meaning higher water concentration produces higher diffusion rates (Ni and Zhang, 2008). Information about water abundance, distribution, and speciation can consequently help to untangle the record of competing geologic processes preserved in volcanic glasses.

We discovered S-shaped enrichments of molecular water in rhyolitic glasses preserved within quartz-hosted embayments from the Mesa Falls Tuff, Yellowstone Plateau volcanic field, western United States (Fig. 1A). Embayments are glass-filled channels that tunnel into crystal interiors (Figs. 1B and 1C). The crystal host partially shields the entrapped melt from subsequent modification, with exchange only allowed via the embayment "mouth" at the crystal's surface. During eruptive degassing, diffusion-limited loss of H₂O and CO₂ from embayments produces negative concentration gradients that can be used for geospeedometry of volcanic decompression rates (e.g., Humphreys et al., 2008; Myers et al., 2018). Quartzhosted embayments from the Mesa Falls Tuff preserve negative CO₂ concentration gradients, indicating slow decompressive ascent rates of $10^{\text{--}3.4\,\pm\,0.5}\,\text{MPa}\;\text{s}^{\text{--}1}$ (Befus et al., 2023). Contrary to expectation, H₂O gradients increase toward the embayment mouth. In this study, we demonstrate that positive concentration gradients of H₂O in Mesa Falls fall deposit embayments were produced by diffusion-limited addition of meteoric water over a period of years to decades in response to a hydrothermal system that was established following deposition of the Mesa Falls ignimbrite. Our work suggests that embayment glasses, already a significant avenue for research because they track syneruptive decompression, also present opportunities to constrain the posteruptive history of volcanic deposits.

METHODS AND RESULTS

Quartz crystals were handpicked from gently crushed pumice lapilli and loose bulk aggregate from a Mesa Falls pyroclastic fall deposit (44.122°N, 111.441°W). At this location, the fall deposit is directly overlain by $\sim \! \! 10$ m of Mesa Falls ignimbrite produced from the same eruption. Quartz crystals with glassy embayments were mounted in Crystalbond (Aremco), oriented, and ground and polished to produce a wafer of doubly exposed, doubly polished embayment glass. We analyzed 40 embayments in 39 quartz crystals.

CITATION: Befus, K.S., et al., 2024, Rehydrated glass embayments record the cooling of a Yellowstone ignimbrite: Geology, v. 52, p. 507–511, https://doi.org/10.1130/G51905.1

^{*}kenny.befus@utexas.edu

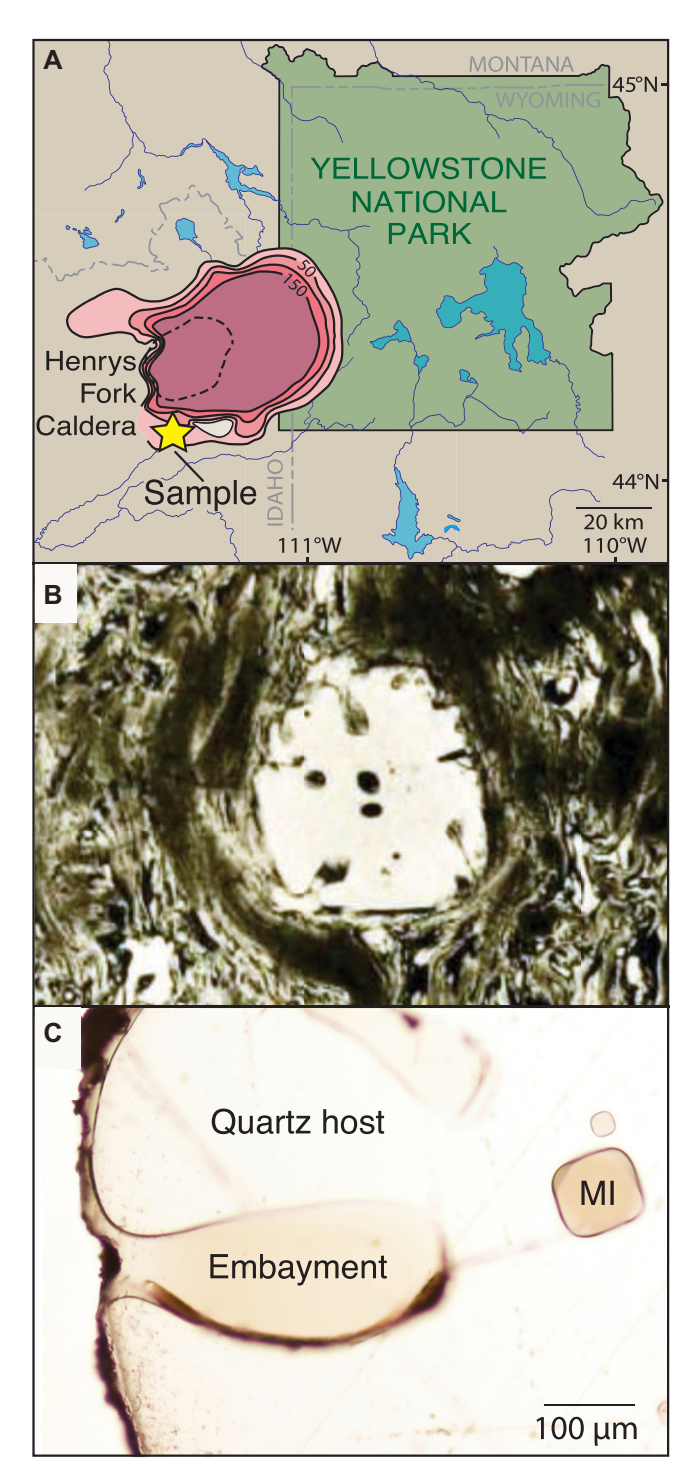


Figure 1. (A) Thickness and extent of Mesa Falls ignimbrite and its source, Henrys Fork caldera (dashed), with isopachs in meters after Christiansen (2001). (B) First description of embayments by Iddings (1899) as "bays of groundmass" in quartz set within welded Yellowstone tuff. (C) Plane-polarized photomicrograph of quartz-hosted embayment from Mesa Falls Tuff (MF-2). MI-glassy melt inclusion. Quartz crystal is \sim 1 mm across.

 $L~cm^{-1}~mol^{-1}$ for CO_2 after Behrens et al. (2004) and a speciation-dependent coefficient for H_2O that varied between $\sim\!60$ and $\sim\!80~L~cm^{-1}~mol^{-1}$ (see Supplemental Material¹). Molecular H_2O was calculated using absorbance at 1630 cm⁻¹

and converted into concentration using an absorption coefficient of 55 L cm⁻¹ mol⁻¹ (Newman et al., 1986). Sample thicknesses, ranging from $\sim\!30$ to 160 μm , were measured in multiple spots along the embayment length using a petrographic microscope equipped with a linear drive encoder. Thickness uncertainties ranged up to 6 μm , and we used that 2σ uncertainty to establish error bars for volatile data.

Mesa Falls Tuff embayments preserve concentration gradients of H₂O and CO₂. CO₂ contents follow standard diffusion-limited gradients that decrease toward the embayment mouth (Supplemental Material). The form of the decreasing CO₂ was produced during eruptive decompression, and it was not altered by rehydration (Befus et al., 2023). The distribution of H₂O is similar across all embayments. Embayment interiors preserve flat, consistent H_2O concentrations ranging from 0.72 ± 0.10 to 1.04 ± 0.10 wt%. These interior concentrations are composed of both hydroxyl and molecular H_2O in roughly equal proportion (54% \pm 10%). Those relatively uniform interior concentrations reflect equilibrium speciation during cooling from magmatic temperatures. The interiors ramp into steep, S-shaped rehydration fronts in the final 50-135 μm closest to the embayment mouth (Fig. 2). Rehydration fronts are enriched up to $1.73 \pm 0.06 - 3.17 \pm 0.10$ wt% H₂O. Most of the water in those enrichments occurs as molecular H_2O (82% \pm 5%). Such high molecular H₂O is a disequilibrium speciation produced by low-temperature rehydration.

GEOSPEEDOMETER MODEL

The diffusion-limited form of the rehydration fronts in the Mesa Falls pyroclastic fall embayments can be used as a geospeedometer, one that presents the opportunity to extract the cooling time scale of the subsequent landscapealtering Mesa Falls ignimbrite. Geospeedometers exploit some geochemical signatures of the time scale of a volcanic process (e.g., Wallace et al., 2003; Lavallée et al., 2015). Here, time-temperature information is preserved in the S-shaped rehydration fronts, which are superimposed upon concentration gradients originally produced during volcanic decompression. To model the rehydration process, we assumed the relatively flat, consistent H₂O gradients in the embayment interiors represent the initial condition for rehydration. The one-dimensional (1-D) finite-difference script, its description, and boundary conditions are provided in the Supplemental Material.

The diffusivity of H_2O in rhyolite glass $(D_{\rm H2O})$ expected in a cooling ignimbrite is one variable that must be established. Both archaeologic and volcanic research concurs that $D_{\rm H2O}$ is $\sim 10^{-23.5\pm0.5}\,{\rm m^2\,s^{-1}}$ in dry rhyolite glass at ambient conditions at Earth's surface (\sim 0.1 wt% H_2O ; Liritzis and Laskaris, 2011; Giachetti et al.,

^{&#}x27;Supplemental Material. Summary of H_2O contents of the embayments, Figures S1–S2, and Tables S1–S2. Please visit https://doi.org/10.1130/GEOL .S.25439152 to access the supplemental material; contact editing@geosociety.org with any questions. The algorithm developed to model the diffusion caused by rehydration can be found at https://doi.org/10.5281/zenodo.10171874.

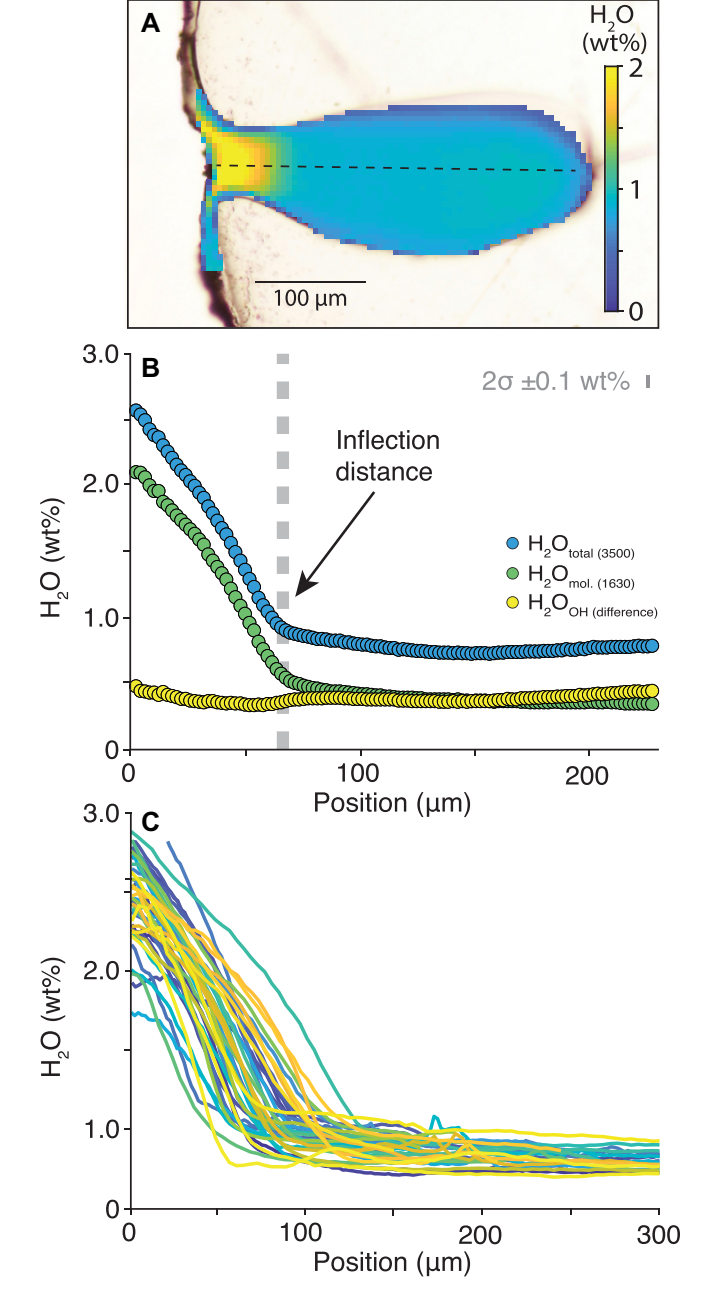


Figure 2. (A, B) Water distribution in quartz-hosted embayment measured with synchrotron Fourier transform infrared spectroscopy (FTIR) and 3 μ m spatial resolution (MF-2 as in Fig. 1C). Dashed line in A shows transect in B. (C) Compilation of transects demonstrates range and similarity of rehydration across all samples (n=40).

2020). It is also accepted that $D_{\rm H2O}$ will increase with increasing temperature and/or increasing water concentration. In experiments, >400 °C, D_{H2O} increases linearly with H₂O contents up to 1.8-2 wt% (Ni and Zhang, 2008; Coumans et al., 2020). The proportionality becomes exponential as water contents increase further (Zhang and Ni, 2010). It is the exponential relationship that produces the S shapes observed here, as well as those described in Yellowstone perlites and hydrothermal experiments (Bindeman and Lowenstern, 2016; Hudak and Bindeman, 2020). We suggest the formulation by Ni and Zhang (2008) is the best available approach for modeling $D_{\rm H2O}$ in rhyolite glasses <400 °C, although their work specifically constrained diffusivity across the interval of \sim 400 to \sim 1600 °C (Ni and Zhang,

2008). Extrapolating the data presented by Ni and Zhang (2008) down from 400 °C to 0 °C reveals two important results: (1) It maintains the appropriate Arrhenian form, and (2) it predicts $\rm H_2O$ diffusivity of $\rm 10^{-23}$ to $\rm 10^{-24}~m^2~s^{-1}$ at ambient conditions, coinciding with expectation (e.g., Giachetti et al., 2020; Fig. S1).

We emphasize that rehydration modeling does not produce unique solutions but instead matches with observed concentration gradients as joint time-temperature-diffusivity combinations. We assumed the pyroclastic fall cooled to ambient temperatures during deposition, and that no rehydration occurred in the eruption column. We have no direct constraints on the emplacement temperature or cooling rate of the Mesa Falls ignimbrite. Matrix and embay-

ment glasses have not altered to clays, nor have the rhyolite glasses lost alkalis. No columnar alteration was observed (e.g., Self et al., 2022). Together, the absence of those alteration features suggests limited temporal exposure to fluids >100 °C. Diffusivity is better constrained than cooling rate, so we treated the time-temperature path as the primary unknown in our model.

We first calculated the time-temperature path for a cooling ignimbrite using a 1-D finite-difference thermal conductivity model. Conductive cooling presented a cooling time scale for the ignimbrite of \sim 40 yr to return to 5 °C. To establish this time scale, we modeled cooling of a 10-m-thick, crystal-rich rhyolitic ignimbrite as a single sheet. The ignimbrite was emplaced on top of a 5 m fall deposit initially at 5 °C. Bulk porosity (vesicles and interparticle space) was assumed to be 60% for all deposits (e.g., Karstens et al., 2023). Density and thermal conductivity of the solids were assumed to be 2600 kg m^{-3} and 1.6 W m^{-1} K⁻¹ (Sass et al., 1988), respectively, with the effects of porosity accounted for using the model of Bagdassarov and Dingwell (1994). Specific heat was from Lavallée et al. (2015). This model inherently simplifies the cooling system by neglecting liquid and gas flow, the temperature dependence of thermodynamic properties, and possible changes in porosity.

We focused on the form of the time-temperature path for material at \sim 1 m depth within the pyroclastic fall deposit where our samples were collected (Fig. 3B; Fig. S2). Conductive cooling predicts that the samples warmed rapidly in the first months after ignimbrite deposition. After reaching maximum temperatures between 150 °C and 250 °C, samples likely then cooled along an exponentially decreasing trend for the subsequent decades (Fig. 3C). Conductive cooling models have been shown to well approximate the time-temperature paths directly observed in some cooling ignimbrites following their historic eruptions (Riehle et al., 1995; Keating, 2005). When water sourced by precipitation or groundwater transports significant amounts of heat by liquid or vapor flows, cooling can be either faster or slower than the conductive limit depending on position within the ignimbrite (Randolph-Flagg et al., 2017). Here, we neglected cooling by precipitation because it would affect the upper parts of the ignimbrite, and the subsurface under the fall deposits would not reach the boiling temperature of water.

GEOLOGIC SIGNIFICANCE OF THE HYDRATION FRONTS

The Mesa Falls ignimbrite erupted to produce the Henrys Fork caldera at 1.300 ± 0.001 Ma (Rivera et al., 2016). The eruption age represents the maximum diffusive time scale permitted for meteoric rehydration. The region's alpine, glacial-interglacial climate has been largely consistent

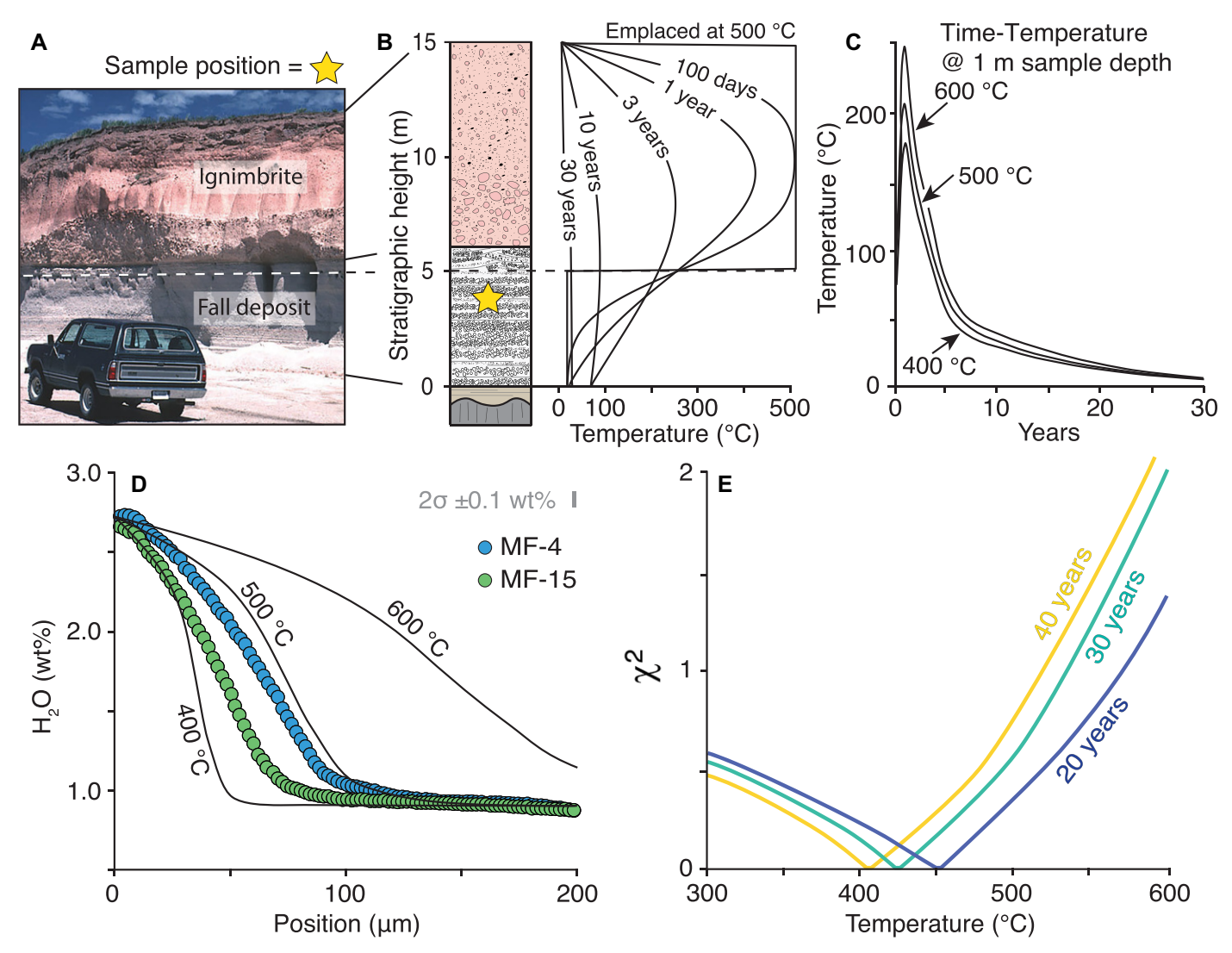


Figure 3. (A) Mesa Falls Tuff outcrop in Ashton Quarry (U.S. Geological Survey image). (B) Measured section of deposit stratigraphy and sampling depth. Pumice, lapilli, and bedding are schematic, with colors chosen to represent outcrop appearance. (C) Conductive cooling model of temperature evolution at sample depth upon deposition of 10-m-thick ignimbrite at varying temperatures. (D) Comparison of transects from samples MF-4 and MF-15 with models produced using 10-m-thick ignimbrite emplaced at various temperatures. (E) Monte Carlo style analyses (χ^2 minima) present best-fit emplacement temperatures for MF-15 assuming different cooling time scales.

since 1.3 Ma. Past climate supplied ample meteoric waters produced by orographic precipitation during cold winters and cool summers (seasonal range of $\sim\!\!-10\,^{\circ}\mathrm{C}$ to $\sim\!10\,^{\circ}\mathrm{C}$; Licciardi and Pierce, 2018). H_2O diffusivity during cold rehydration has been estimated to be $\sim\!10^{-23.5\pm0.5}$ m² s $^{-1}$ (see Giachetti et al., 2020, and references therein), but modeling cold rehydration since the eruption at 1.3 Ma produced enrichments that extend $<\!20\,\mu\mathrm{m}$ into embayments (Fig. S1). Cold rehydration therefore would require impermissibly long diffusive time scales ranging from 10 to 100 m.y. to reproduce the observed gradients.

Rehydration fronts must have been generated by much higher diffusivity. We propose the embayment glasses were instead rehydrated after the ignimbrite transformed the extant cold hydrologic system into a high-temperature hydrothermal system. By analogy, we introduce the Valley of Ten Thousand Smokes,

Alaska. The Griggs expedition first reached Novarupta in 1916, 4 yr after its caldera-forming eruption. They christened a nearby valley as the Valley of Ten Thousand Smokes because "the whole valley as far as the eye could reach was full of hundreds, no thousands—literally tens of thousands—of smokes curling up from the fissured floor." The Valley of Ten Thousand Smokes hydrothermal system remained active for \sim 100 yr (Griggs, 1922; Hogeweg et al., 2005). Year-to-decade hydrothermal systems have been also observed in pyroclastic density current deposits at Mount Pinatubo, Philippines (e.g., Self et al., 2022).

Geospeedometry modeling recovered the penetration distance, enrichment, and S-shaped forms of the observed rehydration fronts in the $\sim\!40$ yr permitted by conductive cooling (Figs. 3D and 3E). Modeling also demonstrated how variations in ignimbrite character can each

influence rehydration. Whereas sample depth and ignimbrite thickness were directly measured, emplacement temperature is unknown. Our observations generated model results that suggest emplacement at 400–450 °C, coinciding with published estimates for unwelded rhyolitic ignimbrites (Figs. 3D and 3E). Equally good fits to the data can be produced at higher temperatures, but only if the ignimbrite cooled faster than expected from pure end-member conductive cooling. More rapid cooling could be produced by effects of latent heat of vaporization. The paleoclimate of the Yellowstone region likely supplied ample groundwater and percolating precipitation to cycle through the cooling ignimbrite and its substrate.

Embayments have a relatively simple geometry that can only be modified across the spatially limited, unprotected mouth. Glass will consequently be preserved in embayments

much longer than other glasses in the same environment. Glass preservation, and its use, is also improved because embayment glasses are commonly dense, which reduces complications associated with vesiculation. Embayment-hosted crystals are emplaced instantaneously by volcanic eruptions that tend to have tight geochronologic constraints. Taken together, glassy embayments may be an as-of-now untapped record for paleoclimate and archaeology that could preserve information in deposits where no other glass remains because of age or other glass degradation processes.

ACKNOWLEDGMENTS

This research used resources of the Advanced Light Source, a U.S. Department of Energy Office of Science User Facility under contract no. DE-AC02-05CH11231. This research was made possible by grants from the National Science Foundation to K. Befus and M. Manga (grants EAR 2015255 and EAR 2042173, respectively). Reviews by Thomas Giachetti and Iona McIntosh improved this manuscript.

REFERENCES CITED

- Anovitz, L.M., Cole, D.R., and Fayek, M., 2008, Mechanisms of rhyolitic glass hydration below the glass transition: The American Mineralogist, v. 93, p. 1166–1178, https://doi.org/10.2138/am .2008.2516.
- Bagdassarov, N., and Dingwell, D., 1994, Thermal properties of vesicular rhyolite: Journal of Volcanology and Geothermal Research, v. 60, p. 179–191, https://doi.org/10.1016/0377-0273(94)90067-1.
- Befus, K.S., Ruefer, A.C., Allison, C.M., and Thompson, J.O., 2023, Quartz-hosted inclusions and embayments reveal storage, fluxing, and ascent of the Mesa Falls Tuff: Yellowstone: Earth and Planetary Science Letters, v. 601, https://doi.org/10.1016/j.epsl.2022.117909.
- Behrens, H., Tamic, N., and Holtz, F., 2004, Determination of the molar absorption coefficient for the infrared absorption band of CO₂ in rhyolitic glasses: The American Mineralogist, v. 89, p. 301–306, https://doi.org/10.2138/am-2004-2-307.
- Bindeman, I.N., and Lowenstern, J.B., 2016, Low- δD hydration rinds in Yellowstone perlites record rapid syneruptive hydration during glacial and interglacial conditions: Contributions to Mineralogy and Petrology, v. 171, 89, https://doi.org/10.1007/s00410-016-1293-1.
- Cassel, E.J., and Breecker, D.O., 2017, Long-term stability of hydrogen isotope ratios in hydrated volcanic glass: Geochimica et Cosmochimica Acta, v. 200, p. 67–86, https://doi.org/10.1016/j.gca.2016.12.001.
- Christiansen, R.L., 2001, The Quaternary and Pliocene Yellowstone Plateau Volcanic Field of Wyoming, Idaho, and Montana: U.S. Geological Survey Professional Paper 729-G, 145 p., https://doi.org/10 .3133/pp729G.
- Coumans, J.P., Llewellin, E.W., Humphreys, M.C., Nowak, M., Brooker, R.A., Mathias, S.A., and McIntosh, I.M., 2020, An experimentally-validated numerical model of diffusion and speciation of water in rhyolitic silicate melt: Geochimica

- et Cosmochimica Acta, v. 276, p. 219–238, https://doi.org/10.1016/j.gca.2020.02.026.
- Friedman, I., and Smith, R.L., 1960, A new dating method using obsidian: Part I. The development of the method: American Antiquity, v. 25, p. 476–493, https://doi.org/10.2307/276634.
- Giachetti, T., Hudak, M.R., Shea, T., Bindeman, I.N., and Hoxsie, E.C., 2020, D/H ratios and H₂O contents record degassing and rehydration history of rhyolitic magma and pyroclasts: Earth and Planetary Science Letters, v. 530, https://doi.org/10.1016/j.epsl.2019.115909.
- Griggs, R.F., 1922, The Valley of Ten Thousand Smokes: Washington, D.C., National Geographic Society, 341 p., https://doi.org/10.5962/bhl.title.43899.
- Hogeweg, N., Keith, T.E.C., Colvard, E.M., and Ingebritsen, S.E., 2005, Ongoing hydrothermal heat loss from the 1912 ash-flow sheet, Valley of Ten Thousand Smokes, Alaska: Journal of Volcanology and Geothermal Research, v. 143, p. 279–291, https://doi.org/10.1016/j.jvolgeores.2004.12.003.
- Hudak, M.R., and Bindeman, I.N., 2020, Solubility, diffusivity, and O isotope systematics of H₂O in rhyolitic glass in hydrothermal temperature experiments: Geochimica et Cosmochimica Acta, v. 283, p. 222–242, https://doi.org/10.1016/j.gca .2020.06.009.
- Hudak, M.R., Bindeman, I.N., Loewen, M.W., and Giachetti, T., 2021, Syn-eruptive hydration of volcanic ash records pyroclast-water interaction in explosive eruptions: Geophysical Research Letters, v. 48, https://doi.org/10.1029 /2021GL094141.
- Humphreys, M.C., Menand, T., Blundy, J.D., and Klimm, K., 2008, Magma ascent rates in explosive eruptions: Constraints from H₂O diffusion in melt inclusions: Earth and Planetary Science Letters, v. 270, p. 25–40, https://doi.org/10.1016/j.epsl.2008.02.041.
- Iddings, J.P., 1899, The rhyolites, in Hague, A., et al., eds., Geology of the Yellowstone National Park Part II—Descriptive Geology, Petrography, and Paleontology: U.S. Geological Survey Monograph 32, p. 356–432, https://doi.org/10.3133/m32.
- Karstens, J., et al., 2023, Revised Minoan eruption volume as benchmark for large volcanic eruptions: Nature Communications, v. 14, p. 2497, https://doi.org/10.1038/s41467-023-38176-3.
- Keating, G.N., 2005, The role of water in cooling ignimbrites: Journal of Volcanology and Geothermal Research, v. 142, p. 145–171, https://doi.org/10.1016/j.jvolgeores.2004.10.019.
- Lavallée, Y., et al., 2015, Eruption and emplacement timescales of ignimbrite super-eruptions from thermo-kinetics of glass shards: Frontiers of Earth Science, v. 3, https://doi.org/10.3389/feart .2015.00002.
- Licciardi, J.M., and Pierce, K.L., 2018, History and dynamics of the Greater Yellowstone Glacial System during the last two glaciations: Quaternary Science Reviews, v. 200, p. 1–33, https://doi.org/10.1016/j.quascirev.2018.08.027.
- Liritzis, I., and Laskaris, N., 2011, Fifty years of obsidian hydration dating in archaeology: Journal of Non-Crystalline Solids, v. 357, p. 2011–2023, https://doi.org/10.1016/j.jnoncrysol.2011.02.048.
- McIntosh, I.M., Aoki, K., Yanagishima, T., Kobayashi, M., Murata, M., and Suzuki, T., 2022, Reconstruction of submarine eruption processes from FTIR volatile analysis of marine tephra: Exam-

- ple of Oomurodashi volcano, Japan: Frontiers of Earth Science, v. 10, https://doi.org/10.3389/feart.2022.963392.
- Mitchell, S.J., McIntosh, I.M., Houghton, B.F., Carey, R.J., and Shea, T., 2018, Dynamics of a powerful deep submarine eruption recorded in H₂O contents and speciation in rhyolitic glass: The 2012 Havre eruption: Earth and Planetary Science Letters, v. 494, p. 135–147, https://doi.org/10.1016/j.epsl.2018.04.053.
- Myers, M.L., Wallace, P.J., Wilson, C.J., Watkins, J.M., and Liu, Y., 2018, Ascent rates of rhyolitic magma at the onset of three caldera-forming eruptions: The American Mineralogist, v. 103, p. 952–965, https://doi.org/10.2138/am-2018-6225.
- Newman, S., Stolper, E.M., and Epstein, S., 1986, Measurement of water in rhyolitic glasses: Calibration of an infrared spectroscopic technique: The American Mineralogist, v. 71, p. 1527–1541.
- Ni, H., and Zhang, Y., 2008, H₂O diffusion models in rhyolitic melt with new high pressure data: Chemical Geology, v. 250, p. 68–78, https://doi .org/10.1016/j.chemgeo.2008.02.011.
- Randolph-Flagg, N., Breen, S., Hernandez, A., Manga, M., and Self, S., 2017, Evenly spaced columns in the Bishop Tuff (California, USA) as relicts of hydrothermal cooling: Geology, v. 45, p. 1015– 1018, https://doi.org/10.1130/G39256.1.
- Riehle, J.R., Miller, T.F., and Bailey, R.A., 1995, Cooling, degassing and compaction of rhyolitic ash flow tuffs: A computational model: Bulletin of Volcanology, v. 57, p. 319–336, https://doi.org/10.1007/BF00301291.
- Rivera, T.A., Schmitz, M.D., Jicha, B.R., and Crowley, J.L., 2016, Zircon petrochronology and ⁴⁰Ar/³⁹Ar sanidine dates for the Mesa Falls Tuff: Crystal-scale records of magmatic evolution and the short lifespan of a large Yellowstone magma chamber: Journal of Petrology, v. 57, p. 1677–1704, https://doi.org/10.1093/petrology/egw053.
- Sass, J.H., Lachenbruch, A.H., Dudley, W.W., Jr., Priest, S.S., and Munroe, R.J., 1988, Temperature, Thermal Conductivity, and Heat Flow near Yucca Mountain, Nevada: Some Tectonic and Hydrologic Implications: U.S. Geological Survey Open-File Report 87-649, 118 p., https://doi.org /10.3133/ofr87649.
- Self, S., Randolph-Flagg, N., Bailey, J.E., and Manga, M., 2022, Exposed columns in the Valles caldera ignimbrites as records of hydrothermal cooling, Jemez Mountains, New Mexico, USA: Journal of Volcanology and Geothermal Research, v. 426, https://doi.org/10.1016/j.jvolgeores.2022 107536
- Stolper, E., 1982, The speciation of water in silicate melt: Geochimica et Cosmochimica Acta, v. 46, p. 2609–2620, https://doi.org/10.1016/0016-7037(82)90381-7.
- Wallace, P.J., Dufek, J., Anderson, A.T., and Zhang, Y., 2003, Cooling rates of Plinian-fall and pyroclastic-flow deposits in the Bishop Tuff: Inferences from water speciation in quartz-hosted glass inclusions: Bulletin of Volcanology, v. 65, p. 105– 123, https://doi.org/10.1007/s00445-002-0247-9.
- Zhang, Y., and Ni, H., 2010, Diffusion of H, C, and O components in silicate melts: Reviews in Mineralogy and Geochemistry, v. 72, p. 171–225, https://doi.org/10.2138/rmg.2010.72.5.

Printed in the USA